Chem. Senses 32: 783–794, 2007
doi:10.1093/chemse/bjm046
Advance Access publication July 18, 2007

Long-Term Modifications in the Strength of Excitatory Associative Inputs in the Piriform Cortex

Andrew Young[1,2] and Qian-Quan Sun[1,2]

[1]Department of Zoology and Physiology and [2]Neuroscience Program, University of Wyoming, Laramie, WY 82071, USA

Correspondence to be sent to: Qian-Quan Sun, Neuroscience Program, University of Wyoming, Laramie, WY 82071, USA. e-mail: neuron@uwyo.edu

Abstract

Afferent olfactory information, in vivo and in vitro, can be rapidly adapted to through a metabotropic glutamate receptor (mGluR)–mediated attenuation of synaptic strength. Specific cellular and synaptic mechanisms underlying olfactory learning and habituation at the cortical level remain unclear. Through whole-cell recording, excitatory postsynaptic currents (EPSCs) were obtained from piriform cortex (PC) principal cells. Using a coincidental, pre- and postsynaptic stimulation protocol, long-term depression (LTD) in synaptic strength was induced at associative, excitatory synapses onto layer II pyramidal neurons of the mouse (P15-27) PC. LTD was mimicked and occluded by mGluR agonists and blocked by nonselective mGluR antagonist (RS)-α-methyl-4-sulfonophenylglycine (MSPG) but not by *N*-methyl-D-aspartic acid (NMDA) receptor antagonist 2-amino-5-phosphonovaleric acid (APV). Analysis of the paired-pulse ratio, α-amino-3-hydroxy-5-methyl-4-isoxazolepropionic acid (AMPA)/NMDA current ratio, and spontaneous EPSCs indicate that electrically induced LTD was mediated predominantly by postsynaptic mechanisms. Additionally, presynaptic mGluRs were involved in agonist-mediated synaptic depression. Immunohistochemical analysis supports the presence of multiple subclasses of mGluRs throughout the PC, with large concentrations of several receptors present in layer II. These observations provide further evidence of activity-dependent, long-term modification of associative inputs and its underlying mechanisms. Cortical adaptation at associative synapses provides an additional link between cortical olfactory processing and subcortical centers that influence behavior.

Key words: association inputs, habituation, mGluR, olfaction, piriform cortex

Introduction

Within the olfactory system, a key component of cortical information processing is the ability of the piriform cortex (PC) to incorporate odorant cues from thousands of olfactory receptors into myriad cortical and subcortical regions. Olfaction, in particular, relies heavily upon feedforward and feedback signaling from diverse, subcortical structures including the amygdala and the hypothalamus (Motokizawa et al. 1985; Price et al. 1991) in order to affect an organism's behavior. These subcortical areas are in close communication with the principal pyramidal neurons of layer II of the PC, through an extensive network of association fibers. A physiologically curious property of olfactory processing is that, in mammals, odorants can be adapted to at an extremely rapid rate, while, within the same system, long-lasting odorant memories can trigger biological responses crucial to an animal's survival (Sullivan 2003; Moriceau and Sullivan 2004). Previous studies have found that afferent olfactory information, both in vivo and in vitro, can be rapidly adapted to through a metabotropic glutamate receptor (mGluR)–mediated attenuation of synaptic strength (Best and Wilson 2004). Current thinking dictates that adaptation allows the cortex to selectively respond to changes in stimuli and suppress background or extraneous sensory information (Kadohisa and Wilson 2006). The synaptic and cellular mechanisms that mediate these properties are unclear at specific piriform cortical circuits. However, alterations in synaptic strength are thought to be the functional hallmark of learning, according to Hebbian-style rules.

Cortical sensory systems provide a unique opportunity to examine the plasticity of neural circuits. The PC, in particular, provides a unique model system due to its 3-layered cytoarchitecture and the fact that signals from the periphery reach the cortex without the need for a precortical, thalamic relay (see Shepherd 2005 for a review). Another advantage is the clear segregation between primary sensory afferent fibers of the lateral olfactory tract (LOT) and the extensive network of

association fibers that link the PC to numerous cortical and subcortical structures. Through the isolation of these inputs, it becomes possible to examine associative circuitry independent of primary sensory afferent input. This study was primarily concerned with the question of how cortical olfactory information is incorporated into subcortical, ''association'' areas of the brain. An understanding of this phylogenetically old region may allow comparisons to be made with the known mechanisms of neocortical sensory regions and further our understanding of cortical microcircuits.

Numerous studies have shown that discriminative olfactory learning can modify PC circuitry in a profound and long-lasting fashion (Saar et al. 2002; Franks and Isaacson 2005), but evidence of specific mechanisms is lacking. There is also considerable data regarding long-term synaptic alterations in the PC following various forms of electrical stimulation (Jung et al. 1990; Kanter and Haberly 1990). Hebbian-style learning describes increases or decreases in synaptic strength depending upon the coincidental activity of pre- and postsynaptic neurons. We utilized methods to elicit synaptic alterations through an established protocol: coincidental pre- and postsynaptic paired stimulation. Through the pairing of associational fiber (located in layer III) stimulation and single-cell somatic action potentials, we were able to generate long-term depression (LTD) of excitatory synapses onto principal, layer II pyramidal neurons of the PC. This procedure carries the obvious advantage of electrophysiologically isolating a single principal neuron and its associational fiber in layer III for study. Through the use of various pharmacological agents, the pairing-dependent LTD was found to be mediated by mGluRs, *N*-methyl-D-aspartic acid (NMDA) receptor independent, and reliably induced through the use of mGluR agonists.

Materials and methods

Brain slice preparation and electrophysiological recordings

All brain slices were prepared in the following manner. C57Bl6 (P15-27) mice were deeply anesthetized and decapitated. The brains were quickly removed and placed into cold (~4 °C) oxygenated slicing medium containing (in mM) 2.5 KCl, 1.25 NaH_2PO_4, 10.0 $MgCl_2$, 0.5 $CaCl_2$, 26.0 $NaHCO_3$, 11.0 glucose, and 234.0 sucrose. Coronal tissue slices (250–300 μm) were cut using a vibratome (TPI, St Louis, MO), transferred to a holding chamber, and incubated (35 °C) for at least 1 h. Individual slices were then transferred to a recording chamber, fixed to a modified microscope stage, and allowed to equilibrate for at least 30 min before recording. Slices were minimally submerged and continuously superfused with oxygenated physiological saline at the rate of 4.0 ml/min. The physiological perfusion solution contained (in mM) 126.0 NaCl, 2.5 KCl, 1.25 NaH_2PO_4, 1.0 $MgCl_2$, 2.0 $CaCl_2$, 26.0 $NaHCO_3$, and 10.0 glucose. Solutions were gassed with 95% O_2/5% CO_2 to a final pH of 7.4 at a temperature of 35 ± 1 °C. A high-powered water immersion objective (63×) with Nomarski optics and infrared video was used to visualize individual neurons. Recording pipettes were fabricated from capillary glass obtained from World Precision Instruments (Sarasota, FL; M1B150F-4), using a Sutter Instrument P80 puller, and had tip resistances of 2–5 MΩ when filled with the intracellular solutions below. A Multiclamp 700B amplifier (Molecular Devices, Foster City, CA) was used for voltage-clamp and current-clamp recordings. Patch pipette saline was composed of (in mM) 130 K-gluconate, 10.0 phosphocreatine–Tris, 3.0 $MgCl_2$, 0.07 $CaCl_2$, 4-ethylene glycol tetraacetic acid, 10.0 4-(2-hydroxyethyl)-1-piperazineethanesulfonic acid, 4.0 Na_2-ATP, and 1.0 Na-GTP, pH adjusted to 7.4 and osmolarity adjusted to 280 $mosMl^{-1}$. For recording NMDA-mediated currents, the K-gluconate was replaced by Cs K-gluconate. Neurobiotin (0.5%; Vector Laboratories, Burlingame, CA) was regularly added to the patch pipette solution. Data were accepted for analysis when access resistance in whole-cell recordings ranged from 5 to 8 MΩ and was stable (<25% change) during the recording. The resting membrane potential and the resting input resistance of the cell were also monitored to ensure a stable baseline recording. Current- and voltage-clamp protocols were generated using PCLAMP9.2 software (Molecular Devices). A sharpened bipolar tungsten electrode, placed at ~50 μm away from recorded cells in the cortical layer III, was used to activate association fibers of the PC (Figure 1A). Monosynaptic excitatory postsynaptic currents (EPSCs) were evoked in pyramidal neurons and were recorded at a holding potential of either −80 or +20 mV (in order to isolate α-amino-3-hydroxy-5-methyl-4-isoxazolepropionic acid (AMPA) receptor–mediated or NMDA receptor–mediated glutamatergic currents, respectively, (Figure 1). All evoked excitatory post-synaptic currents (eEPSCs) were evoked in the presence of a cocktail artificial cerebrospinal fluid solution containing $GABA_A$ antagonist picrotoxin (50 μM) and a low concentration of AMPA/kainite receptor antagonist 2,3-dihydro-6-nitro-7-sulfamoyl-benzo(F) quinoxaline (NBQX; 0.1 μM) to reduce excitation and prevent hyperexcitability (Kumar and Huguenard 2001) (e.g., Figure 1B). The paired-pulse ratio (PPR) of evoked events was quantified by evoking 2 EPSCs 200 ms apart. The second event was divided by the first event and averaged at specific time points across multiple recordings.

Chemicals: GYK1 52466 hydrocloride (Sigma-Aldrich, St Louis, MO); NBQX (Tocris, Ellisville, MO), DL-AP5 (Tocris), and SR95531 (Tocris). Selective agonist for mGluRs (Tocris), (±)-*trans*-ACPD: [(±)-1-aminocyclopentane-*trans*-1,3-dicarboxylic acid, group I/II mGlu receptors]; (RS)-3,5-DHPG: [(RS)-3,5-dihydroxyphenylglycine; group I metabotropic agonist]; selective antagonist for mGluRs: AIDA: [(RS)-1-aminoindan-1,5-dicarboxylic acid; selective antagonist of group I metabotropic]; LY341495: [(2S)-2-amino-2-[(1S,2S)-2-carboxycycloprop-1-yl]-3-(xanth-9-yl]

propanoic acid; selective antagonist of group II metabotropic]; MSPG: [(RS)-α-methyl-4-sulfonophenylglycine; a relatively nonselective antagonist of mGlu receptors]. APV: 2-amino-5-phosphonovaleric acid, NMDA receptor antagonist.

Pre- and postsynaptic pairing protocol

Coincident presynaptic and postsynaptic long-term plasticity induction protocols are adopted from established protocols (Bi and Poo 2001; Dan and Poo 2004). Prior to the pairing induction, a minimum of 30 min of control baseline recording is performed. The induction protocol consists of repetitive presynaptic stimulation at 1 Hz each followed (10-ms interval) by a postsynaptic spike induced by injection of depolarizing current pulses for 5 min. Experiments are continued only when a stable baseline amplitude is observed prior to induction. The change in synaptic current amplitudes was evaluated for all time points following the pairing period, normalized to the baseline eEPSC amplitude and presented as scatter plots. Three time points (5, 30, and 60 min) were chosen to be presented as bar graphs in order to provide a quantitative representation of the data. Data were analyzed using the paired *t*-test to compare pretreatment to posttreatment groups. All data are presented as ±standard error of mean.

Immunohistochemistry

At postnatal day 30, mice were given a lethal injection of Nembutal and perfused intracardially with 0.1 M sodium phosphate buffer, pH 7.4, followed by 4% paraformaldehyde. The brain was then removed, and the whole cortex was dissected. The tissue was cryoprotected in 30% sucrose and then cut into 40-μm-thick parasagittal sections. Sections were incubated in 0.6% H_2O_2 for 30 min; phosphate-buffered saline (PBS) washed; switched to 50% alcohol for 10 min; PBS washed; then incubated in TBS with 0.5% Triton X-100, 2% bovine serum albumin, and 10% normal goat serum for 2 h; and incubated in primary antibodies directed against mGluR1 (1:500, Chemicon, Billerica, MA), mGluR2/3 (1:500, Chemicon), mGluR5 (1:500, Chemicon), and mGluR8 (1:500, Chemicon) overnight. The next day, after PBS rinsing, sections were incubated in Alexa Fluor 594, goat anti-mouse IgG (H + L) for PV for 3 h, then rinsed, mounted, and coverslipped. The immunofluorescent specimens were examined using an epifluorescence microscope (Carl Zeiss, Thornwood, NY) equipped with AxioCam digital color camera. Confocal microscopy images were sampled using an upright Nikon E800 microscope and Bio-Rad Radiance 2100 image analysis software suits.

Results

Whole-cell patch clamp recordings were made in layer II pyramidal neurons (Figure 1A). EPSCs were elicited by electrically stimulating layer III "association fibers" and isolated pharmacologically (Figure 1). Using a coincidental stimulation protocol to stimulate the association fibers while depolarizing the recorded pyramidal neurons (Materials and Methods), we found that robust LTD of excitatory synaptic transmission was elicited after low-frequency coincidental presynaptic and postsynaptic stimulations (Figure 2A1). One, relatively brief period (5 min) of pre- and postsynaptic

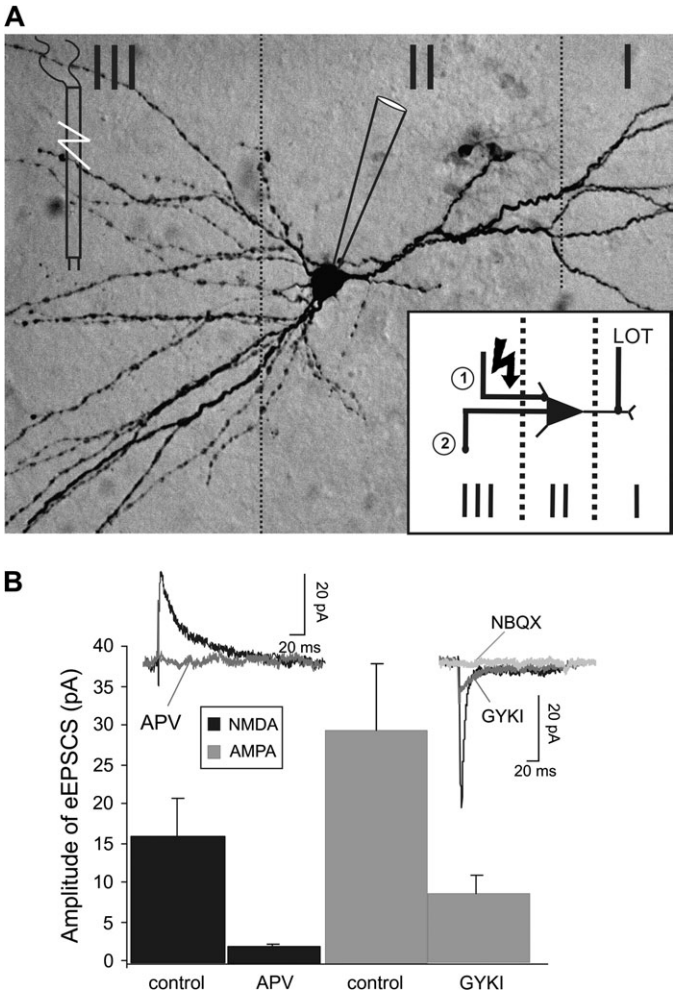

Figure 1 Whole-cell recording from layer II pyramidal neurons and pharmacological isolation of EPSCs. **(A)** Representation of the recording/stimulation configuration in the PC. Recordings and postsynaptic current injections were made from the soma of pyramidal neurons located in layer II, whereas the stimulating electrode was placed ~50 μm away in layer III. Scale bar: 30 μm. Inset: Simplified schematic of the PC circuit under investigation. 1) Association fiber. 2) To subcortical areas. **(B)** Top: A representative recording of eEPSCs from the cell shown in (A). The eEPSCs were recorded at different membrane potentials (−80 mV or +20 mV) in order to isolate AMPA- or NMDA-mediated currents, respectively. Note the effects that NMDA receptor antagonist APV (50 μM), the AMPA receptor antagonist GYKI (100 μM), and the AMPA/kainate receptor antagonist NBQX (50 μM) have upon their respective currents. Bottom: Bar graph showing the amplitudes of averaged AMPA- or NMDA-mediated currents and the effects of the NMDA receptor antagonist APV and the selective AMPA receptor antagonist GYKI on their respective currents.

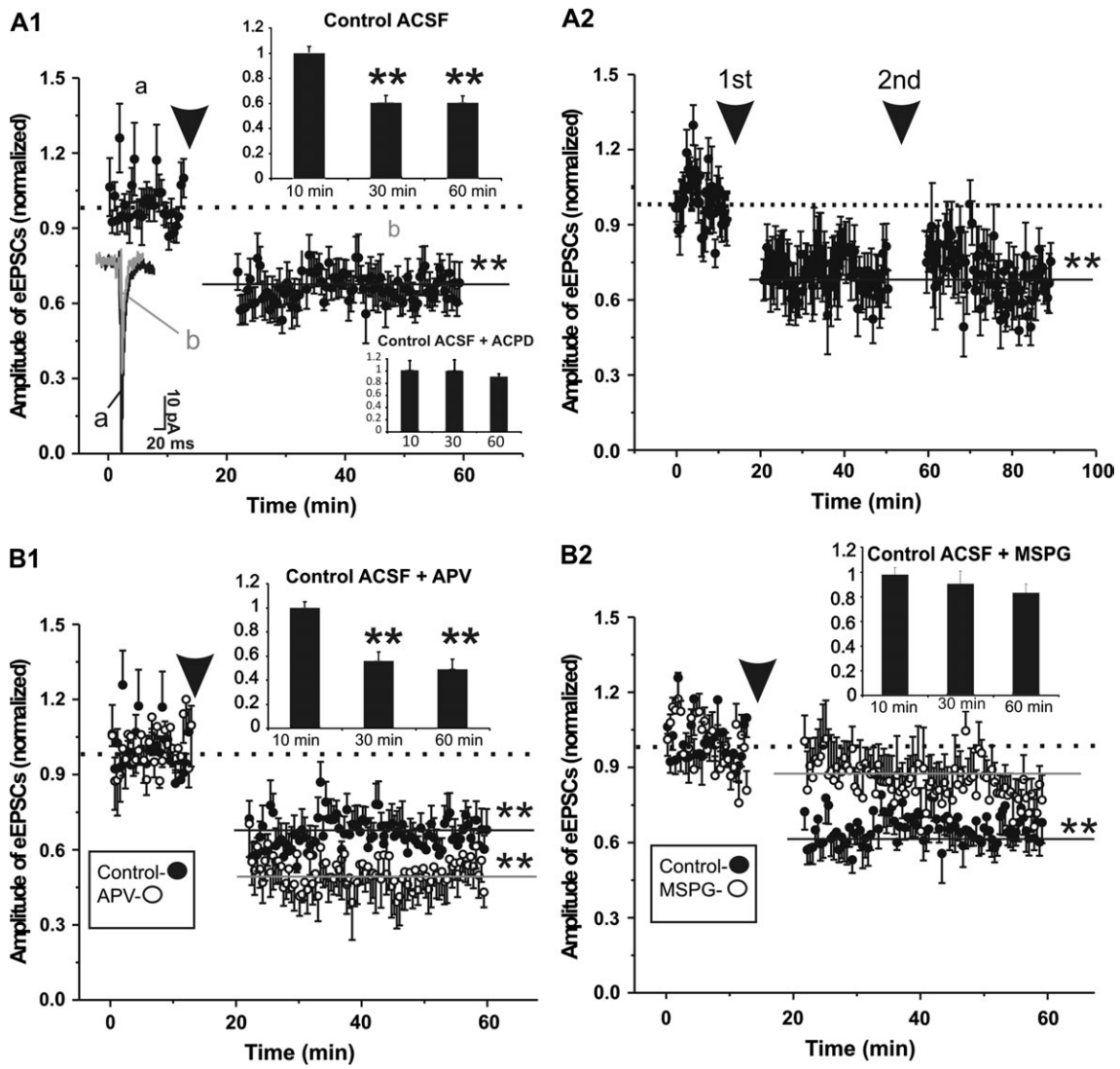

Figure 2 Induction of LTD following coincidental pre- and postsynaptic stimulation. **(A)** Normalized amplitude values prior to and following the electrical stimulation. **(A1)** LTD induced from one, 5-min period of coincidental pre- and postsynaptic stimulation. Representative traces of eEPSC, recorded prior to (a) and following (b) the electrical pairing protocol, are also included (inset, $n = 10$). Inset upper right: Bar graph representation of the average amplitude shift over the recording period are included for control pairing (60% ± 5% of baseline at 60 min). Inset lower right: Bar graph representation of the average amplitude shift over the recording period in the presence of 100 μM *trans*-ACPD (91% ± 5% of baseline at 60 min, $n = 5$). Arrowhead in this and all panels: coincidental pairing at 1 Hz. Dotted line in this and all panels: level of mean amplitude of the eEPSCs during the prepairing period. **(A2)** LTD induction following two, 5-min periods of coincidental pre- and postsynaptic stimulation. Note the lack of cumulative effects following 2 consecutive electrical induction attempts. **(B1)** Normalized amplitude values, comparing electrical induction in control perfused brain slices and slices in the presence of NMDA antagonist APV (100 μM). Note that the LTD induced by electrical induction is independent of NMDA receptor function. Inset: Bar graph representation of the average amplitude shift (49% ± 9% of baseline at 60 min). **(B2)** MSPG (100 μM), a group II/III mGluR antagonist, markedly reduces LTD when perfused during the electrical induction ($n = 7$). Inset: Bar graph representation of the average amplitude shift (84% of baseline ± 8%, $n = 6$). Solid black lines: level of mean amplitude of eEPSCs during the postpairing period of controls (A1), (B1), and (B2) and double-paired controls (A2). Solid gray lines: level of mean amplitude of the eEPSCs during the postpairing period in the presence of antagonists MSPG (B2) or APV (B1). $^{**}P < 0.01$.

coincidental stimulation led to a long-lasting attenuation of synaptic strength, as measured by eEPSC amplitudes (Figure 2A1, upper bar graph, 60% ± 5% of baseline at 60 min, $n = 10$; $P < 0.01$ post- vs. prestimulation). In addition, the synaptic attenuation was not increased following 2 consecutive treatments, indicating a strong ceiling effect for the LTD (Figure 2A2). We first performed occlusion experiments, where 100 μM *trans*-ACPD (Alexander et al. 2007) was added to the bath perfusion at the time of electrical pairing, which show a complete lack of LTD (Figure 2A1, lower bar graph, 91% ± 5% of baseline at 60 min, $n = 5$, $P > 0.1$). This result suggests that receptors or downstream second messengers activated by *trans*-ACPD were involved in the LTD. Next, we examined whether the LTD can be blocked

by pharmacological agents. To determine whether the induced LTD was dependent upon the function of NMDA receptors, the NMDA antagonist, APV (100 μM), was administered via bath perfusion. The pairing protocol, performed in the presence of APV, demonstrated an insignificant increase in the synaptic attenuation when compared with controls (Figure 2B1, 49% ± 9% of baseline at 60 min, $n = 6$; $P < 0.01$ pre- vs. poststimulation). To determine whether the induced LTD was being mediated by mGluRs, the mGluR antagonist MSPG (100 μM) was applied locally. MSPG attenuated the electrically induced LTD (Figure 2B2, 83% ± 7% of baseline at 60 min, $n = 7$, $P > 0.1$), when compared with control experiments. These results suggest that the LTD is mediated via mGluR and not via NMDA receptors.

Next, we examined whether there was a correlation between the ability to induce LTD and the effects of exogenously applied mGluR agonists. The group I/II mGluR agonist *trans*-ACPD (100 μM) was capable of producing synaptic depression of similar magnitude to that seen upon electrical induction (Figure 3A1, 58% ± 7% of baseline at 30 min, $n = 9$; $P < 0.01$ post- vs. prestimulation), but with a slight washout effect not seen following electrical induction (Figure 3A1, 63% ± 18% of baseline at 60 min). Compared with the electrically induced LTD, *trans*-ACPD administration induced a similar degree of attenuation on the amplitude of the eEPSCs (Figures 3A1 vs. 2A1). Group I mGluR agonist DHPG (100 μM) (Alexander et al. 2007) had similar effects to *trans*-ACPD and the synaptically evoked LTD (Figure 3A2, 51% ± 13% of baseline at 60 min, $n = 7$; $P < 0.01$ pre- vs. postagonist application). Application of mGluR antagonists in the bath perfusion was successful in blocking the pharmacologically induced synaptic depression. Potent group II antagonist LY-341495 (100 μM), while incapable of completely blocking the agonist-induced depression at 30 min (Figure 3B1 [black bars], 79% ± 12% of baseline, $n = 10$; $P < 0.05$), was capable of completely blocking the depression after 60 min (Figure 3B1, 94% ± 10% of baseline, $n = 10$), as was the group I antagonist AIDA (100 μM, Figure 3B2, 95% ± 26% of baseline at 60 min, $n = 6$). Due to the previously reported lack of group II specificity of LY-341495 at μM doses, we also perfused the antagonist at 100 nM, finding similar results (Figure 3B1 [gray bar] 98% ± 16% of baseline at 60 min, $n = 5$). Thus, these data suggest the strong possibility that pharmacologically induced synaptic depression was induced through the actions of multiple mGluRs and that, with the inclusion of the MSPG data, both electrically and pharmacologically induced synaptic alterations are mediated by mGluR-dependent mechanisms. To determine whether presynaptic or postsynaptic mechanisms were involved in these synaptic alterations, we measured the AMPA/NMDA ratio, which has been widely used to determine the mechanisms of LTD (Thomas et al. 2001). Using *trans*-ACPD as our agonist of choice for the induction of synaptic depression, we isolated different excitatory postsynaptic receptor–mediated currents in order to determine their relative contributions to the depression. Using whole-cell, voltage-clamp experiments (with Cs^+ pipette solution), the resting membrane potential (Vm) was varied in order to isolate both AMPA- and NMDA-mediated currents in the same layer II pyramidal neuron (Kumar and Huguenard 2001). With a Vm of −80, only AMPA currents were recorded (with contributions from a small number of putative kainate receptors attenuated by 50 μM NBQX perfusion, Figure 1B). At Vm of +20, only NMDA-mediated currents were recorded (verified pharmacologically, cf. Figure 1B). The results showed that there was a reduction in both AMPA- and NMDA-mediated current amplitudes following administration of *trans*-ACPD (Figure 4A1, $n = 9$). However, the reduction in NMDA-mediated current is substantially smaller than the reduction in AMPA-mediated current (Figure 4A1). Upon comparing the ratio of AMPA receptor– versus NMDA receptor–mediated current, prior to and following administration of *trans*-ACPD, we found that there was a small but very significant decrease in the ratio (Figure 4A2, $P < 0.01$, $n = 9$). These results indicate that a postsynaptic reduction in AMPA receptors, possibly due to receptor endocytosis (Holman et al. 2006), was largely responsible for the mGluR-mediated synaptic depression. In addition, these results do not rule out that there were inhibitory effects on presynaptic glutamate release as well.

We also monitored the PPR before, during, and after the application of (±)-*trans*-ACPD, DHPG, and coincidental stimulation. The PPR showed a significant ($P < 0.01$) increase following administration of both mGluR agonists *trans*-ACPD (100 uM) and DHPG (100 uM) (Figure 5A2, $n = 9$ [*trans*-ACPD] and 7 [DHPG]). The increase in the PPR was blocked when the agonists were perfused with both mGluR antagonists (data not shown). Interestingly, the facilitation of the PPR seen upon agonist administration is not found in cells following electrical induction of LTD or electrical induction in the presence of APV or MSPG (Figure 5A1, $n = 10$, 6, and 7, respectively). This indicates that a postsynaptic mechanism, similar to that reported in cerebellar cells (Chung et al. 2003; Zhang and Linden 2006) and hippocampal neurons (Bredt and Nicoll 2003), mediates the effects. However, additional presynaptic receptors appear to be recruited by the agonists (ACPD and DHPG). Analysis of spontaneous EPSCs (sEPSCs) indicates that there were significant ($P < 0.01$, $n = 5$) deceases in both sEPSC amplitude (Figure 5B1, from 6.3 ± 1.2 pA to 4.1 ± 0.5 pA) and frequency (Figure 5B2, from 9.1 ± 1.8 Hz to 5.7 ± 0.48 Hz) following *trans*-ACPD administration. However, only sEPSC amplitude shows a significant return to pre-ACPD levels during the washout period (Figure 5B1, from 4.1 pA ± 0.5 to 4.9 pA ± 1.8). Alterations in the amplitude and frequency of sEPSCs suggest the involvement of both pre- and postsynaptic *trans*-ACPD–mediated effects.

Lastly, immunohistochemical analysis was used to determine which mGluR receptors were localized in the PC.

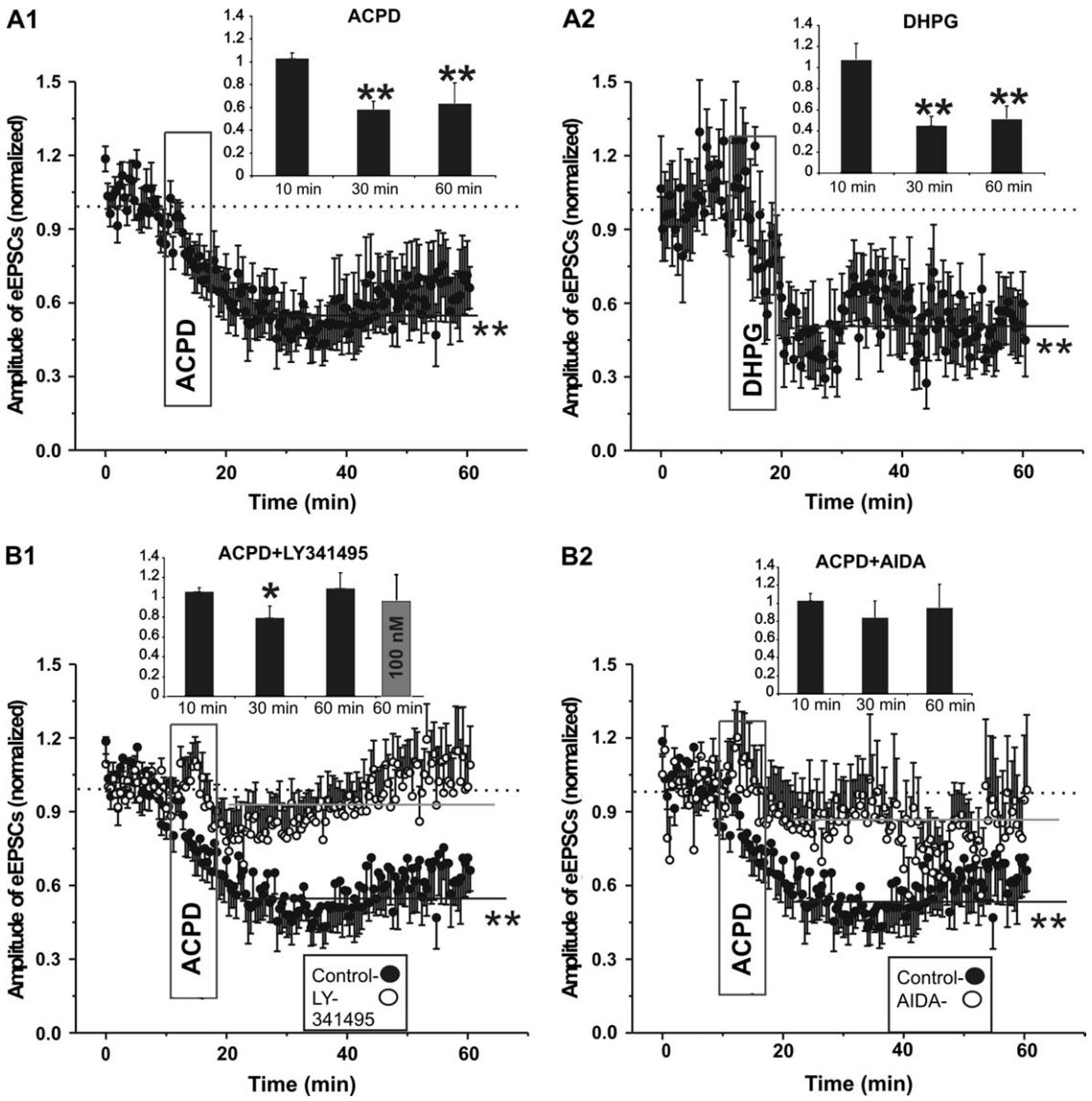

Figure 3 Synaptic depression following mGluR agonist administration. **(A1)** Normalized amplitudes of eEPSCs prior to and following the administration of *trans*-ACPD (100 μM), a group I/II mGluR agonist. Note that while synaptic depression is induced, there is a partial return to baseline eEPSC amplitude after a relatively short length of time. Inset: Bar graph representation of the average amplitude shift (63% ± 18% of baseline at 60 min). **(A2)** Normalized amplitudes of eEPSCs prior to and following the administration of DHPG (100 μM), a group I mGluR agonist. Note the rapid and large synaptic depression and the subsequent partial recovery to baseline amplitudes. Inset: Bar graph representation of the average amplitude shift (51% ± 13% of baseline at 60 min.). Solid black line: level of mean amplitude of the eEPSCs at the postpairing period. Dotted line in this and all panels: level of mean amplitude of the eEPSCs at the prepairing period. **(B1)** Note the marked reduction in *trans*-ACPD–induced synaptic depression when it is coadministered with group II mGluR antagonist, LY 341495 (100 μM). Inset: Bar graph representation of the average amplitude shift following *trans*-ACPD administration in the presence of 100 μM LY 341495 (black bars, 94% ± 10% of baseline at 60 min) and 100 nM (gray bar, 98% ± 16% of baseline at 60 min). **(B2)** Selective group I mGluR antagonist AIDA (100 μM) is also capable of virtually abolishing the *trans*-ACPD–induced synaptic depression. Inset: Bar graph representation of the average amplitude shift (95% ± 26% of baseline at 60 min). Solid black lines: level of mean amplitude of eEPSCs during the postpairing period following administration of mGluR agonists *trans*-ACPD (A1), (B1), and (B2) and DHPG (A2). Solid gray lines: level of the mean amplitude of eEPSCs duirng the postpairing period following the administration of mGluR agonist *trans*-ACPD in the presence of LY 341495 (B1) or AIDA (B2). $*P < 0.05$, $**P < 0.01$.

Antibodies against mGluRs belonging to each of the 3 major groups of mGluRs (groups are based upon sequence similarity, pharmacology, and intracellular signaling mechanisms) I, II, and III were used to pinpoint the cellular location of the mGluRs. mGluR1-IR and mGluR5-IR (groups I) are shown in Figures 6A and C, respectively. There were abundant mGluR1-IR–positive fibers running from deep layers III through II (Figure 6A). mGluR2/3-IRs (group II) are shown in Figure 6B. mGluR8-IRs (group III) are shown in Figure 6D. Each of these receptors were found throughout the PC

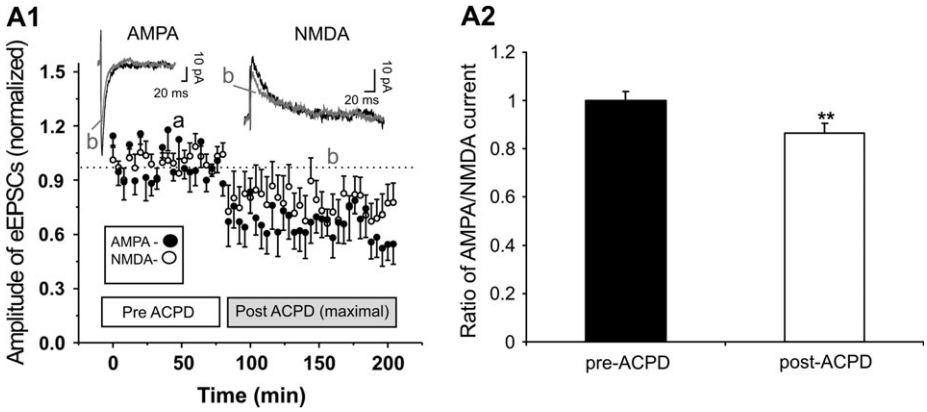

Figure 4 Contribution of AMPA and NMDA currents to synaptic depression. **(A1)** Normalized amplitudes of eEPSCs prior to and following the administration of *trans*-ACPD (100 μM, $n = 10$). AMPA- and NMDA-mediated currents were isolated by adjusting the resting membrane potential using the voltage-clamp configuration. These currents were confirmed through the use of pharmacological agents (see Figure 1B). Note the smaller reduction in NMDA-mediated eEPSCs when compared with AMPA-mediated currents. Representative traces of AMPA- and NMDA-mediated currents both before (a) and after (b) *trans*-ACPD administration (inset). Dotted line: level of mean amplitude of the eEPSCs at the prepairing period. **(A2)** Graph representing the ratio of AMPA-mediated current plotted against the NMDA-mediated current. Note a small but significant change in the AMPA/NMDA receptor–mediated currents ratio after the pairing. $^{**}P < 0.01$ ($n = 10$).

and were especially concentrated in layer II. Using immunohistochemical double-labeling techniques, we found that mGluR1-IR was expressed abundantly at both presynaptic sites (white arrowheads in Figure 7A) and in the postsynaptic membrane, opposed to the glutamatergic varicosities in principal neurons (yellow arrowheads in Figure 7A). The cellular pattern of mGluR8-IR in these cells was slightly different, that is, the majority of the mGluR8-IR was found in the glutamatergic presynaptic varicosities (white arrowheads in Figure 7B). These results are consistent with the involvement of multiple mGluRs in the formation of LTD and in the presynaptic and postsynaptic signaling of associative fibers in the PC.

Discussion

Long-term synaptic modifications are hallmarks of numerous integral central nervous system (CNS) processes (Borgland et al. 2004; Monfils and Teskey 2004). Memory and learning are 2 of the cognitive/functional applications thought to be mediated by LTD and its counterpart, long-term potentiation (LTP). LTP and LTD, terms that represent a suite of inducible changes in synaptic strength, are thought to be an important method for encoding information in the CNS. Various brain regions, most prominently the hippocampus, have been closely studied in order to determine the function and mechanisms pertaining to LTD (Stein et al. 2003; Morishita et al. 2005). In addition, LTD has been found in numerous sensory systems, including somatosensory (Bender et al. 2006) and visual (Choi et al. 2005). In the PC, it is less clear how information is encoded, at both the synaptic and circuitry levels. Several studies have investigated long-term changes in PC circuitry but have primarily focused on how learned behavior modifies synaptic plasticity (both LTP and LTD) (Lebel et al. 2001; Truchet et al. 2002; Brosh and Barkai 2004). The mechanisms that underlie previously reported LTD are also unclear. In particular, LTD mediated by mGluRs has only recently received close scrutiny into its possible mechanisms, such as postsynaptic AMPA receptor endocytosis (Bredt and Nicoll 2003; Moult et al. 2006). One of our first findings was the independence of the electrical stimulus–induced LTD from the function of NMDA receptors (Figure 2B1). Similar LTD induction has been reported in CA1 synapses in the hippocampus (which possess both NMDA-dependent and -independent forms of LTD) following the administration of DHPG (Palmer et al. 1997).

This study made use of a relatively refined technique for the induction of LTD, spike-timing coincidental presynaptic stimulation, and postsynaptic depolarizations. For a review of spike-timing plasticity and its relationship with LTD/LTP, see Dan and Poo (2006). This protocol was designed with the purpose of eliciting LTD in primary olfactory cortical neurons, through low-frequency pairing. All experiments were performed in the presence of a pharmacological "cocktail" in order to isolate putative excitatory synaptic events (picrotoxin and NBQX). The cocktail was included in order to block $GABA_A$-mediated inhibitory activity, while preventing the formation of epileptiform activity in the cortex (Kumar and Huguenard 2001). We have shown that exogenous application of mGluR groups I/II agonist *trans*-ACPD attenuated eEPSCs in a magnitude and through a time course similar to synaptically induced LTD. In contrast, NMDA receptor antagonist APV, which blocks LTD in other brain regions (Gean and Lin 1993), did not block the LTD in the PC (Figure 2B1). LTD in other brain regions has been previously shown

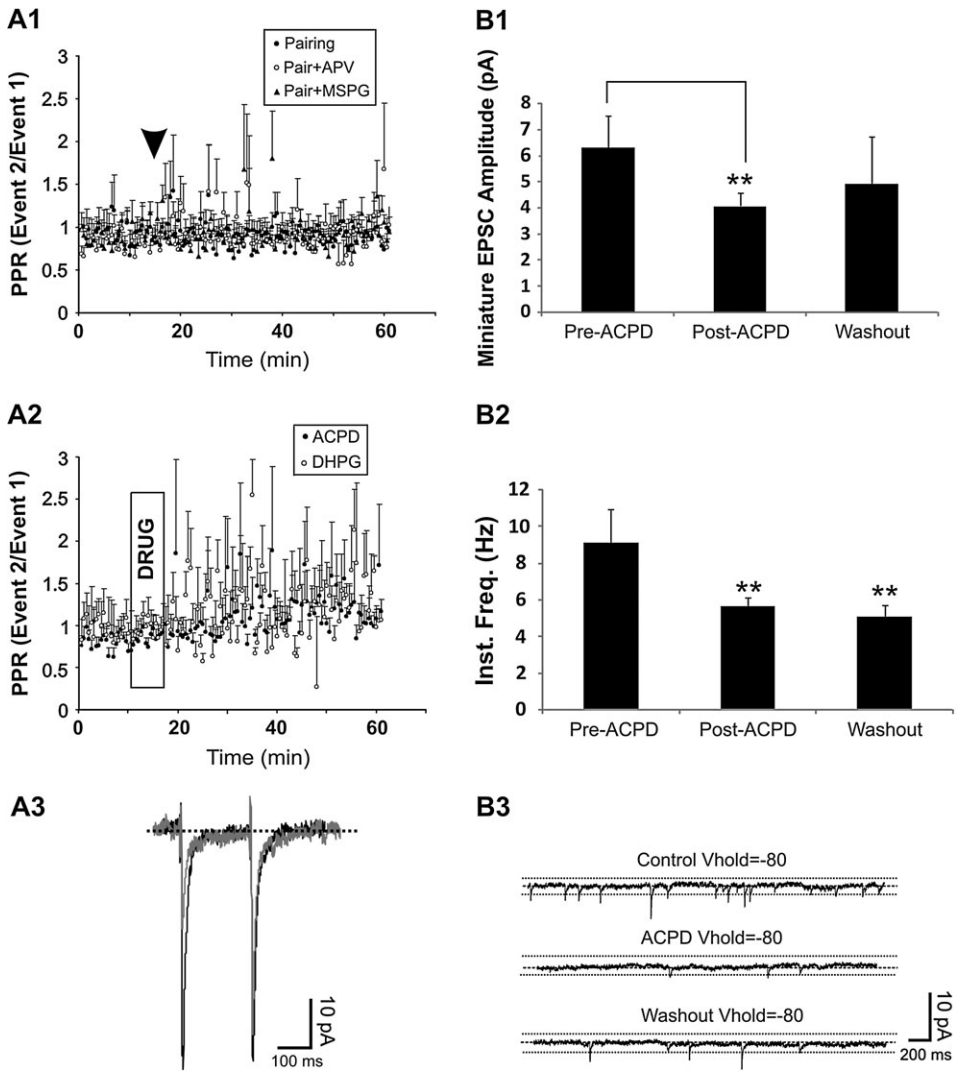

Figure 5 Paired-pulse ratio of eEPSCs and miniature EPSC analysis. **(A1)** The PPR (event 2/event 1, 200-ms interval) of EPSCs induced through electrical pairing (control perfusion or in the presence of MSPG or APV); the large arrowhead indicates the point between the prepairing and postpairing PPR. **(A2)** PPR (event 2/event 1) of EPSCs following administration of mGluR agonists (*trans*-ACPD 100 μM, DHPG 100 μM); both agonists resulted in significant ($P < 0.01$) PPR increases. **(A3)** Representative traces of eEPSCs prior to (black) and following (gray) the administration of *trans*-ACPD. Note the increase in the second EPSC amplitude. **(B1)** Quantitative representation of sEPSC amplitude recorded prior to, following, and after the washout of *trans*-ACPD administration. **(B2)** Quantitative representation of sEPSC frequency recorded prior to, following, and after the washout of *trans*-ACPD. **(B3)** Representative traces from the 3 experimental conditions. $^{**}P < 0.01$.

to be mediated by multiple groups of mGluRs (Harris et al. 2004). The use of group I mGluR agonists (DHPG) and antagonists (AIDA) strongly supports the involvement of group I mGluRs for the pharmacological induction of LTD at PC associative synapses. Group II antagonist LY-341495 successfully blocked the *trans*-ACPD–induced synaptic depression at both low (100 nM) and high (100 μM) concentrations (Figure 3B1). Taken together, these data indicate that multiple mGluR groups are involved in *trans*-ACPD–induced synaptic depression. Additionally, electrically induced LTD following the pre/postsynaptic pairing protocol can be successfully attenuated through the use of mGluR group I/II antagonist MSPG and occluded through the use of the mGluR agonist *trans*-ACPD. These data support a mechanistically similar mode of action between electrically induced LTD and pharmacologically induced synaptic depression at PC association fibers. Additional insights into the mechanisms underlying LTD can be obtained from pharmacological and kinetic analysis of eEPSCs. Change in the PPR is indicative of presynaptic modulation. Our results revealed that the PPR showed a significant increase following mGluR agonist administration (ACPD, DHPG) but that no change occurred following electrical pairing (Figure 5A1,A2), suggesting that the LTD, induced electrically, is largely mediated via postsynaptic mechanisms, whereas the pharmacologically induced synaptic depression is both pre- and postsynaptic in

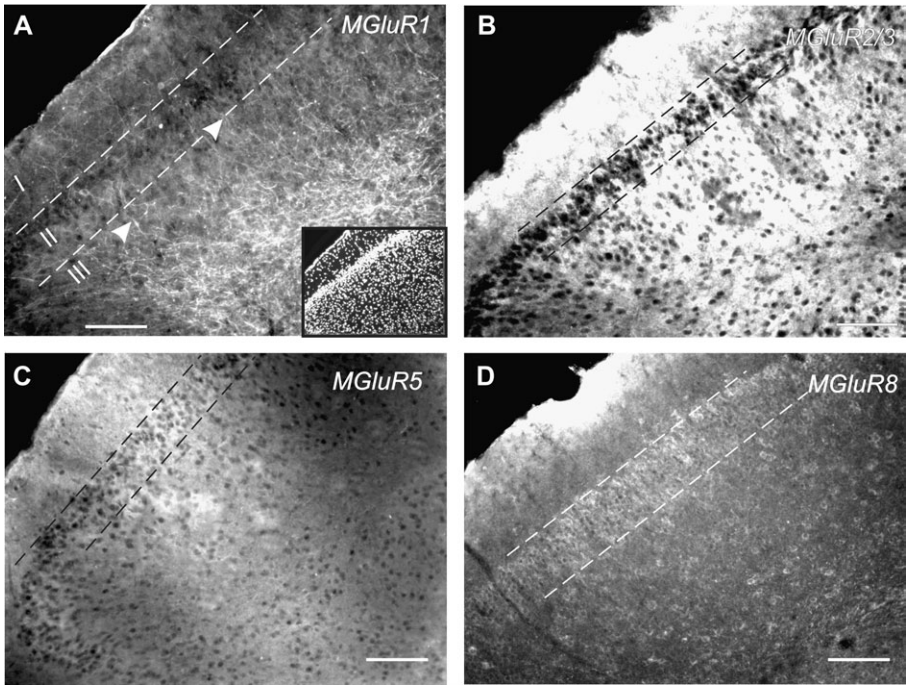

Figure 6 mGluR-IR in the PC. Photomicrograph of the expression of mGlu receptors in the PC. The 4 main groups of mGluRs were stained and visualized: group I **(A, C)**, group II **(B),** and group III **(D)**. Notice the intense localization of the group I receptors-IRs in layer II of the PC and throughout the lower layers. Inset: 4′,6-diamidino-2-phenylindole stained same sections were used to determine laminar location of the mGluR-IRs. Scale bars: 100 μm.

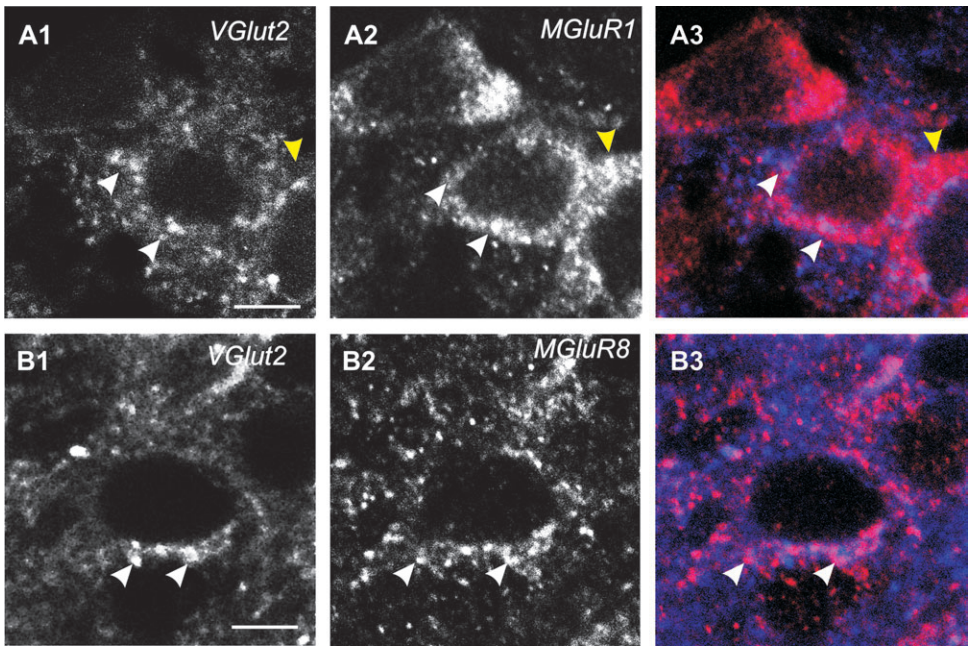

Figure 7 Pre and postsynaptic location of mGluR-IRs in the PC. **(A)** mGluR1-IR and vesicular glutamate transporter 2 (VGlut2)-IR in layer II pyramidal cells. White arrow head: colocalization of the mGluR1 with the vGlut2 at presynaptic varicosities. Yellow: mGluR1-IR in postsynaptic membrane apposing to the presynaptic glutamate varicosities. **(B)** mGluR8-IR and Vglut2-IRs in layer II pyramidal neurons. White arrow head: colocalization at the presynaptic varicosities. Scale bars: 5 μm.

origin. Thus, additional presynaptic receptors were activated by agonist application. Postsynaptic expression of LTD is usually associated with changes in the AMPA/NMDA ratio (Thomas et al. 2001; Bredt and Nicoll 2003). The ratio of AMPA/NMDA decreases following *trans*-ACPD administration, suggesting that changes have occurred at the

postsynaptic level (Figure 4B). Mechanisms similar to those previously reported for AMPA receptor internalization are likely involved (Snyder et al. 2001). However, there is also a small decrease in the amplitude of the NMDA-mediated current, suggesting the possibility of concomitant presynaptic effects. For example, immunohistochemical evidence showed the localization of various mGluRs in the presynaptic varicosities. The reduction in amplitudes of NMDA currents could be due to alterations in presynaptic glutamate release properties (Zakharenko et al. 2002).

The PPR and sEPSC analyses are 2 other means of determining where in a given circuit synaptic alterations are occurring. Previous studies in the PC found that mGluR agonists reduced the amplitude of EPSCs generated by stimulation of the associational fiber pathway of the rat PC, accompanied with paired-pulse facilitation (Tan et al. 2006). This matches well with the observed effects of *trans*-ACPD found in this study. Additionally, Tan et al. (2006) found that group I mGluR agonists showed indications of both pre- and postsynaptic effects upon synaptic transmission, observations supported by our data. In the rat hippocampus, administration of the mGluR agonist DHPG also resulted in an increase in PPR and a decrease in miniature excitatory post-synaptic current frequency, although there was no observed effect upon amplitude (Fitzjohn et al. 2001). These results provide cross-species evidence of the effects mGluR agonists have upon synaptic transmission. Seemingly, whereas electrical pairing involves primarily postsynaptic alterations, mGluR agonist administration involves a combination of pre- and postsynaptic effects.

Our results demonstrated a powerful form of synaptic alteration following brief low-frequency stimulation of associative inputs onto olfactory cortex. Clearly, these synaptic changes have profound implications in regard to how the PC encodes information. Alterations in olfactory circuitry could have broad ramifications for numerous cortical and subcortical regions that respond to and are modified by olfactory experience. Mammalian physiological behaviors, such as respiration, can be significantly influenced by the odorants present in their environment through a signaling system that includes the PC and subsequently subcortical regions such as the amygdala (Onimaru and Homma 2006). Adaptation to sensory stimuli represents a simple form of memory that can occur in various sensory circuits. Current thinking dictates that adaptation allows the cortex to selectively respond to changes in stimuli and suppress background or extraneous sensory information (Kadohisa and Wilson 2006). How does olfactory information alter cortical synapses and how do these alterations affect downstream circuits in diverse brain regions in a long-lasting fashion? It is highly likely that synaptic alterations in the olfactory cortex are at least partially responsible for behavioral responses that stem from cortical adaptive properties, such as habituation.

Previous studies have found that afferent olfactory information, both in vivo and in vitro, can be rapidly adapted to through an mGluR-mediated attenuation of synaptic strength (Best and Wilson 2004). The focus in that study was on the afferent synapses formed between LOT axons and principal neurons of layer II/III PC in the rat. Our results complement this previous work. Here we have demonstrated that, in the mouse, in addition to sensory adaptation occurring at afferent LOT synapses onto principal PC neurons, cortical adaptation (in the form of mGluR-mediated LTD) can also occur between associational olfactory fibers and principal cells. This has important implications for the gating of olfactory information between cortical and subcortical structures and, consequently, upon the behavior of the organism itself. Seemingly, adaptation to odorants (as indicated by a reduction in neuronal responsiveness to stimuli) can occur at virtually every step of the olfactory circuit, from the olfactory receptor (Zufall et al. 1991), to the main olfactory bulb (Mair 1982), to the cortex itself (Wilson 1998), and between cortical neurons and their subcortical pathways (this study). This indicates that within the PC, there is the possibility of mGluR-mediated odorant adaptation at multiple levels and synapses, capable of a consecutive refinement in the signaling. Strong links between mGluR-mediated cortical adaptation and behavioral habituation to odors have recently been established at LOT/principal neuron synapses (Yadon and Wilson 2005). Cortical adaptation at associative synapses provides a further link between cortical olfactory processing and subcortical centers that influence behavior.

Excluding the previous examples, compelling data that correlate cortical adaptation with behavioral habituation have been sparse. In studies conducted with human subjects using olfactory conditioning, it was found that odorant conditioning could elicit functional magnetic resonance imaging responses in the amygdala, which were habituated to over time (Gottfried et al. 2002). In the rodent, it has long been known that the PC (as well as other, secondary olfactory structures) sends direct projections to the lateral nucleus of the amygdala (Lledo et al. 2005). The discovery of multiple sites, and receptors for mGluR-mediated synaptic attenuation in the PC, provides a clearer connection between cortical adaptation and behavior. Together, this allows for powerful and possibly context-specific control over the flow of information from the cortex to multiple brain regions that influence behavior. These results provide a strong foundation for future experiments to incorporate in vivo behavioral studies.

Funding

National Institutes of Health–National Center for Research Resources (P20 RRO15553, P20 RR16474-04).

Acknowledgements

We thank Ms. Chunzhao Zhang for excellent assistance in immunohistological processing. The confocal microscopy was performed at the University of Wyoming microscopy core facility.

References

Alexander SP, Mathie A, Peters JA. 2007. Guide to receptors and channels, 2nd edition (2007 Revision). Br J Pharmacol. 150(Suppl 1):S1–S168.

Bender KJ, Allen CB, Bender VA, Feldman DE. 2006. Synaptic basis for whisker deprivation-induced synaptic depression in rat somatosensory cortex. J Neurosci. 26:4155–4165.

Best AR, Wilson DA. 2004. Coordinate synaptic mechanisms contributing to olfactory cortical adaptation. J Neurosci. 24:652–660.

Bi G, Poo M. 2001. Synaptic modification by correlated activity: Hebb's postulate revisited. Annu Rev Neurosci. 24:139–166.

Borgland SL, Malenka RC, Bonci A. 2004. Acute and chronic cocaine-induced potentiation of synaptic strength in the ventral tegmental area: electrophysiological and behavioral correlates in individual rats. J Neurosci. 24: 7482–7490.

Bredt DS, Nicoll RA. 2003. AMPA receptor trafficking at excitatory synapses. Neuron. 40:361–379.

Brosh I, Barkai E. 2004. Learning-induced long-term synaptic modifications in the olfactory cortex. Curr Neurovasc Res. 1:389–395.

Choi SY, Chang J, Jiang B, Seol GH, Min SS, Han JS, Shin HS, Gallagher M, Kirkwood A. 2005. Multiple receptors coupled to phospholipase C gate long-term depression in visual cortex. J Neurosci. 25:11433–11443.

Chung HJ, Steinberg JP, Huganir RL, Linden DJ. 2003. Requirement of AMPA receptor GluR2 phosphorylation for cerebellar long-term depression. Science. 300:1751–1755.

Dan Y, Poo MM. 2004. Spike timing-dependent plasticity of neural circuits. Neuron. 44:23–30.

Dan Y, Poo MM. 2006. Spike timing-dependent plasticity: from synapse to perception. Physiol Rev. 86:1033–1048.

Fitzjohn SM, Palmer MJ, May JE, Neeson A, Morris SA, Collingridge GL. 2001. A characterisation of long-term depression induced by metabotropic glutamate receptor activation in the rat hippocampus in vitro. J Physiol. 537:421–430.

Franks KM, Isaacson JS. 2005. Synapse-specific downregulation of NMDA receptors by early experience: a critical period for plasticity of sensory input to olfactory cortex. Neuron. 47:101–114.

Gean PW, Lin JH. 1993. D-2-amino-5-phosphonovaleate blocks induction of long-term depression of the NMDA receptor-mediated synaptic component in rat hippocampus. Neurosci Lett. 158:170–172.

Gottfried JA, O'Doherty J, Dolan RJ. 2002. Appetitive and aversive olfactory learning in humans studied using event-related functional magnetic resonance imaging. J Neurosci. 22:10829–10837.

Harris SL, Cho K, Bashir ZI, Molnar E. 2004. Metabotropic glutamate receptor signalling in perirhinal cortical neurons. Mol Cell Neurosci. 25: 275–287.

Holman D, Feligioni M, Henley JM. 2006. Differential redistribution of native AMPA receptor complexes following LTD induction in acute hippocampal slices. Neuropharmacology. 144(1):387–394.

Jung MW, Larson J, Lynch G. 1990. Long-term potentiation of monosynaptic EPSPs in rat piriform cortex in vitro. Synapse. 6:279–283.

Kadohisa M, Wilson DA. 2006. Olfactory cortical adaptation facilitates detection of odors against background. J Neurophysiol. 95:1888–1896.

Kanter ED, Haberly LB. 1990. NMDA-dependent induction of long-term potentiation in afferent and association fiber systems of piriform cortex in vitro. Brain Res. 525:175–179.

Kumar SS, Huguenard JR. 2001. Properties of excitatory synaptic connections mediated by the corpus callosum in the developing rat neocortex. J Neurophysiol. 86:2973–2985.

Lebel D, Grossman Y, Barkai E. 2001. Olfactory learning modifies predisposition for long-term potentiation and long-term depression induction in the rat piriform (olfactory) cortex. Cereb Cortex. 11:485–489.

Lledo PM, Gheusi G, Vincent JD. 2005. Information processing in the mammalian olfactory system. Physiol Rev. 85:281–317.

Mair RG. 1982. Adaptation of rat olfactory bulb neurones. J Physiol. 326: 361–369.

Monfils MH, Teskey GC. 2004. Induction of long-term depression is associated with decreased dendritic length and spine density in layers III and V of sensorimotor neocortex. Synapse. 53:114–121.

Moriceau S, Sullivan RM. 2004. Unique neural circuitry for neonatal olfactory learning. J Neurosci. 24:1182–1189.

Morishita W, Marie H, Malenka RC. 2005. Distinct triggering and expression mechanisms underlie LTD of AMPA and NMDA synaptic responses. Nat Neurosci. 8:1043–1050.

Motokizawa F, Ino Y, Ohta N, Yasuda N. 1985. The principal pathway from the piriform cortex to the deep amygdaloid nuclei in the cat. Neurosci Res. 3:167–170.

Moult PR, Gladding CM, Sanderson TM, Fitzjohn SM, Bashir ZI, Molnar E, Collingridge GL. 2006. Tyrosine phosphatases regulate AMPA receptor trafficking during metabotropic glutamate receptor-mediated long-term depression. J Neurosci. 26:2544–2554.

Onimaru H, Homma I. 2006. Spontaneous oscillatory burst activity in the piriform-amygdala region and its relation to in vitro respiratory activity in newborn rats. Neuroscience. 52(1):92–99.

Palmer MJ, Irving AJ, Seabrook GR, Jane DE, Collingridge GL. 1997. The group I mGlu receptor agonist DHPG induces a novel form of LTD in the CA1 region of the hippocampus. Neuropharmacology. 36:1517–1532.

Price JL, Slotnick BM, Revial MF. 1991. Olfactory projections to the hypothalamus. J Comp Neurol. 306:447–461.

Saar D, Grossman Y, Barkai E. 2002. Learning-induced enhancement of postsynaptic potentials in pyramidal neurons. J Neurophysiol. 87:2358–2363.

Shepherd GM. 2005. Perception without a thalamus how does olfaction do it? Neuron. 46:166–168.

Snyder EM, Philpot BD, Huber KM, Dong X, Fallon JR, Bear MF. 2001. Internalization of ionotropic glutamate receptors in response to mGluR activation. Nat Neurosci. 4:1079–1085.

Stein V, House DR, Bredt DS, Nicoll RA. 2003. Postsynaptic density-95 mimics and occludes hippocampal long-term potentiation and enhances long-term depression. J Neurosci. 23:5503–5506.

Sullivan RM. 2003. Developing a sense of safety: the neurobiology of neonatal attachment. Ann N Y Acad Sci. 1008:122–131.

Tan Y, Hori N, Carpenter DO. 2006. Electrophysiological effects of three groups of glutamate metabotropic receptors in rat piriform cortex. Cell Mol Neurobiol. 26:915–924.

Thomas MJ, Beurrier C, Bonci A, Malenka RC. 2001. Long-term depression in the nucleus accumbens: a neural correlate of behavioral sensitization to cocaine. Nat Neurosci. 4:1217–1223.

Truchet B, Chaillan FA, Soumireu-Mourat B, Roman FS. 2002. Learning and memory of cue-reward association meaning by modifications of synaptic efficacy in dentate gyrus and piriform cortex. Hippocampus. 12:600–608.

Wilson DA. 1998. Habituation of odor responses in the rat anterior piriform cortex. J Neurophysiol. 79:1425–1440.

Yadon CA, Wilson DA. 2005. The role of metabotropic glutamate receptors and cortical adaptation in habituation of odor-guided behavior. Learn Mem. 12:601–605.

Zakharenko SS, Zablow L, Siegelbaum SA. 2002. Altered presynaptic vesicle release and cycling during mGluR-dependent LTD. Neuron. 35:1099–1110.

Zhang W, Linden DJ. 2006. Long-term depression at the mossy fiber-deep cerebellar nucleus synapse. J Neurosci. 26:6935–6944.

Zufall F, Shepherd GM, Firestein S. 1991. Inhibition of the olfactory cyclic nucleotide gated ion channel by intracellular calcium. Proc Biol Sci. 246:225–230.

Accepted June 24, 2007